Optical Materials 51 (2016) 84–88

Contents lists available at ScienceDirect

Optical Materials

journal homepage: www.elsevier.com/locate/optmat

Stress-induced waveguides in Nd:YAG by simultaneous double-beam irradiation with femtosecond pulses

Gabriel R. Castillo [a,*], Carolina Romero [a], Ginés Lifante [b], Daniel Jaque [b], Feng Chen [c], Óscar Varela [d], Enrique García-García [d], Cruz Méndez [d], Santiago Camacho-López [e], Javier R. Vázquez de Aldana [a]

[a] Laser Microprocessing Group, Universidad de Salamanca, Pl. La Merced SN, 37008 Salamanca, Spain
[b] Fluorescence Imaging Group, Departamento de Física de Materiales, Facultad de Ciencias, Universidad Autónoma de Madrid, Madrid 28049, Spain
[c] School of Physics, Shandong University, 250100 Jinan, Shandong, China
[d] Technical Division, Centro de Láseres Pulsados (CLPU), Parque Científico, 37185 Villamayor, Salamanca, Spain
[e] Departamento de Óptica, División de Física Aplicada, Centro de Investigación Científica y de Educación Superior de Ensenada, Carretera Ensenada–Tijuana No. 3018, Zona Playitas, C.P. 22860, Ensenada, B.C., Mexico

ARTICLE INFO

Article history:
Received 23 October 2015
Received in revised form 16 November 2015
Accepted 17 November 2015
Available online 28 November 2015

Keywords:
Laser materials processing
Waveguides channeled
Integrated optics devices

ABSTRACT

We report on the fabrication of stress-induced waveguides in Nd:YAG (neodymium doped yttrium aluminum garnet, Nd:$Y_3Al_5O_{12}$) by simultaneous double-beam irradiation with femtosecond laser pulses. An interferometer was used to generate two femtosecond laser beams that, focused with certain lateral separation inside the crystal, produced two parallel damage tracks with a single scan. The propagation of the mechanical waves simultaneously created in both focal spots produced a highly symmetrical stress field that is clearly revealed in micro-luminescence maps. The optical properties of the double-beam waveguides are studied and compared to those of single-beam irradiation, showing relevant differences. The creation of more symmetric stress patterns and a slight reduction of propagation losses are explained in terms of the fact that simultaneous inscription allows for a drastic reduction in the magnitude of "incubation" effects related to the existence of pre-damaged states.

1. Introduction

Optical waveguides are the basic elements for building integrated photonic devices [1], such as beam splitters, directional couplers or mirroring modulators. In this field, versatile guiding structures with diverse geometries are needed, operating both in the passive as active regimes. Femtosecond laser inscription has been demonstrated to be a very powerful technique for the fabrication of optical waveguides in transparent dielectrics [2–6]. The laser is strongly focused inside the material and the large intensity reached in the focal volume creates a localized modification mediated by non-linear absorption (strong-field ionization) [7]. The ultrashort laser-matter interaction time (femtoseconds) avoids the generation of thermal effects and, as a result, a highly localized material modification is induced. As the focal spot can be scanned inside the material, in principle, any arbitrary 3D structure can be inscribed in it.

The material modifications that can be induced by the laser are classified in Type I or Type II, depending on whether the irradiation conditions are below or above the optical damage threshold, respectively [8]. In crystals [4], the most usual technique for producing waveguides, the so-called *double-line* approach, is based on Type II modifications [9]. In this approach, two parallel laser-damage lines are created close to each other, resulting in a refractive index increase in the area between both lines, due to the stress-field (lattice compression) induced by the ultrashort pulse irradiation, and in a refractive index decrease at the damage lines related to a local amorphization [10]. This technique has been applied to a large number of crystals for the fabrication of different active photonic devices, for instance waveguide lasers [11–14] or wavelength converters [15,16]. Recently, some novel fabrication approaches based on stress-induced optical waveguides have been reported [17–19], offering improved features over the standard double-line technique.

In this work we report on the fabrication and the study of stress-induced optical waveguides in Nd:YAG crystal produced by the simultaneous irradiation of the sample with two femtosecond laser beams generated with an interferometer. The optical paths for both pulsed beams were equalized in order to get simultaneous irradiation of the corresponding pulses. The technique of bifocal inscription, based on the use of a diffractive grating setup,

* Corresponding author.
E-mail address: grcastillo@usal.es (G.R. Castillo).

http://dx.doi.org/10.1016/j.optmat.2015.11.025
0925-3467/

was previously demonstrated in [20] and it was applied to quartz and phosphate glass, showing the possibility to fabricate single-mode waveguides for a wide range of focal separations. However, to the author's knowledge, there is no previous systematic comparative study showing the differences of double-beam irradiation waveguides with the "traditional" double-scan waveguides, including micro-luminescence maps to analyze the damage and stress fields induced during fabrication. The stress fields created by both simultaneous pulses overlap in space and time in the region between the damage tracks, thus obtaining, in all the cases, a symmetrical modification of the refractive index. Moreover, the simultaneous inscription leads to the disappearance of the "incubation" effects caused by the existence of pre-damaged volumes. Thus, the waveguides fabricated with this approach exhibit highly symmetrical modes for a wide range of irradiation conditions, and better performance than the double-scan waveguides.

2. Experimental setup

2.1. Waveguide fabrication

An amplified Ti:sapphire femtosecond laser system (Spitfire Ace, Spectra Physics) was used to inscribe the waveguides in the crystals. The laser emitted 120 fs pulses at a central wavelength of 800 nm with a repetition rate of 1 kHz. A half-wave plate followed by a linear polarizer, and a calibrated neutral density filter, were used to finely tune the pulse energy. An interferometer with a variable delay line was arranged to produce two collinear beams with nearly equalized mean power (see Fig. 1). The optical paths of both beams were adjusted in order to get the best temporal overlap (delay 0 between pulses of the two beams) by optimizing the contrast of the produced interference patterns. Both beams were focused through a 20× microscope objective at 100 μm beneath the sample surface, which was placed on a computer-controlled motorized three-axis stage. The use of an interferometer instead of the diffractive-grating approach reported in [20] allows a fine and continuous control on the focal separation. Eventually, the interferometer would allow the introduction of an arbitrary delay between both pulses if required.

Two sets of experiments were completed: the one, with simultaneous double beam (DB) irradiation, and the other with single beam (SB) irradiation (standard fabrication technique). In the first one (DB), both beams were slightly misaligned (symmetrically, with less than 0.25° of divergence) in the interferometer in order to get two separated focal spots after the microscope objective, with the distance required between them in each experiment (15 μm, 20 μm or 30 μm). The experiments were done in Nd:YAG that is one of the most widely used gain media for solid-state lasers due to its outstanding fluorescence, thermal and mechanical properties. Nd:YAG has been the subject of a number of previous studies on optical waveguide inscription with femtosecond lasers [12,19] and it is very well characterized. The sample was cut to dimension $10 \times 10 \times 2$ mm^3 and polished down to optical quality. The beams were focused inside the crystal through one of the largest faces at a depth of 150 μm. The sample was then scanned once at constant velocity resulting in two parallel damage tracks simultaneously written in the crystal in a single step. In the second set of experiments (SB), one of the beams was blocked in the interferometer, and then, two parallel scans of the sample were done with the other beam in order to produce two parallel damage tracks at the same separation than in the corresponding DB experiment. In both DB as SB experiments, different scanning velocities (25–100 μm/s) and pulse energies (0.2–0.9 μJ) were used in order to explore the effect of the laser irradiation parameters on the waveguide performances.

2.2. Optical waveguide characterization

The modal profiles of the fabricated waveguides were investigated with an end-fire coupling setup at 633 nm. Light at input face of the waveguides was polarized parallel to the inscribed tracks in order to minimize transmission losses (see Fig. 2). The modes at the output face of the waveguide were imaged onto a CCD camera through a microscope objective. Waveguide propagation losses were evaluated by measuring the output and input powers, taking into account losses at the input and output microscope lenses, Fresnel reflections at the crystal interfaces, and the modal overlap between the injected light and the modal profile [21] (linear absorption at the sample was neglected). The refractive

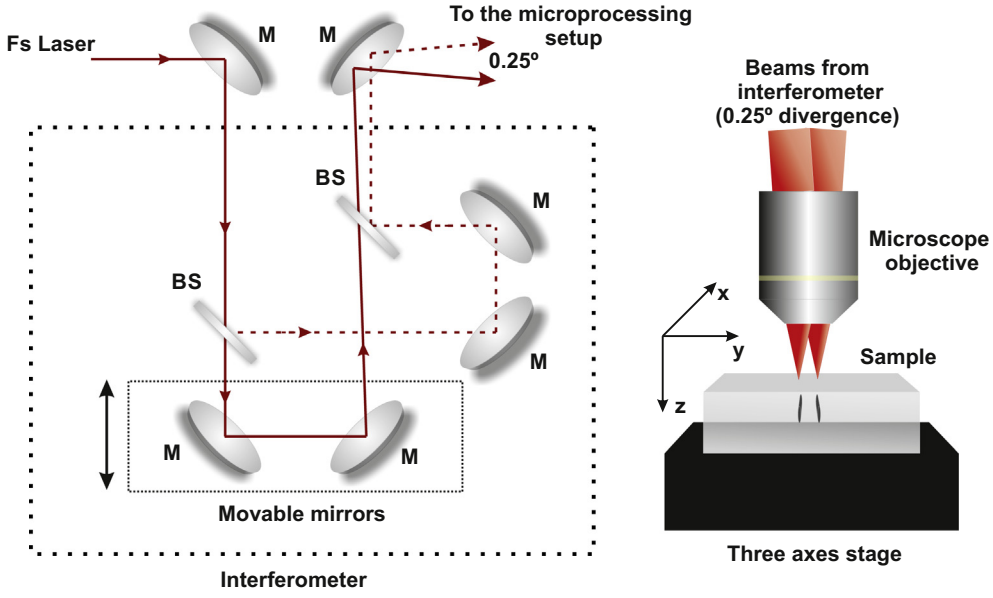

Fig. 1. Schematic of the simultaneous DB irradiation experiments. (a) Interferometer that produces the two beams (M: mirrors, BS: 50–50 beam-splitter). (b) The two beams focused through the microscope objective inside the crystal. (The divergence between the two beams has been exaggerated in the pictures for the sake of clarity.)

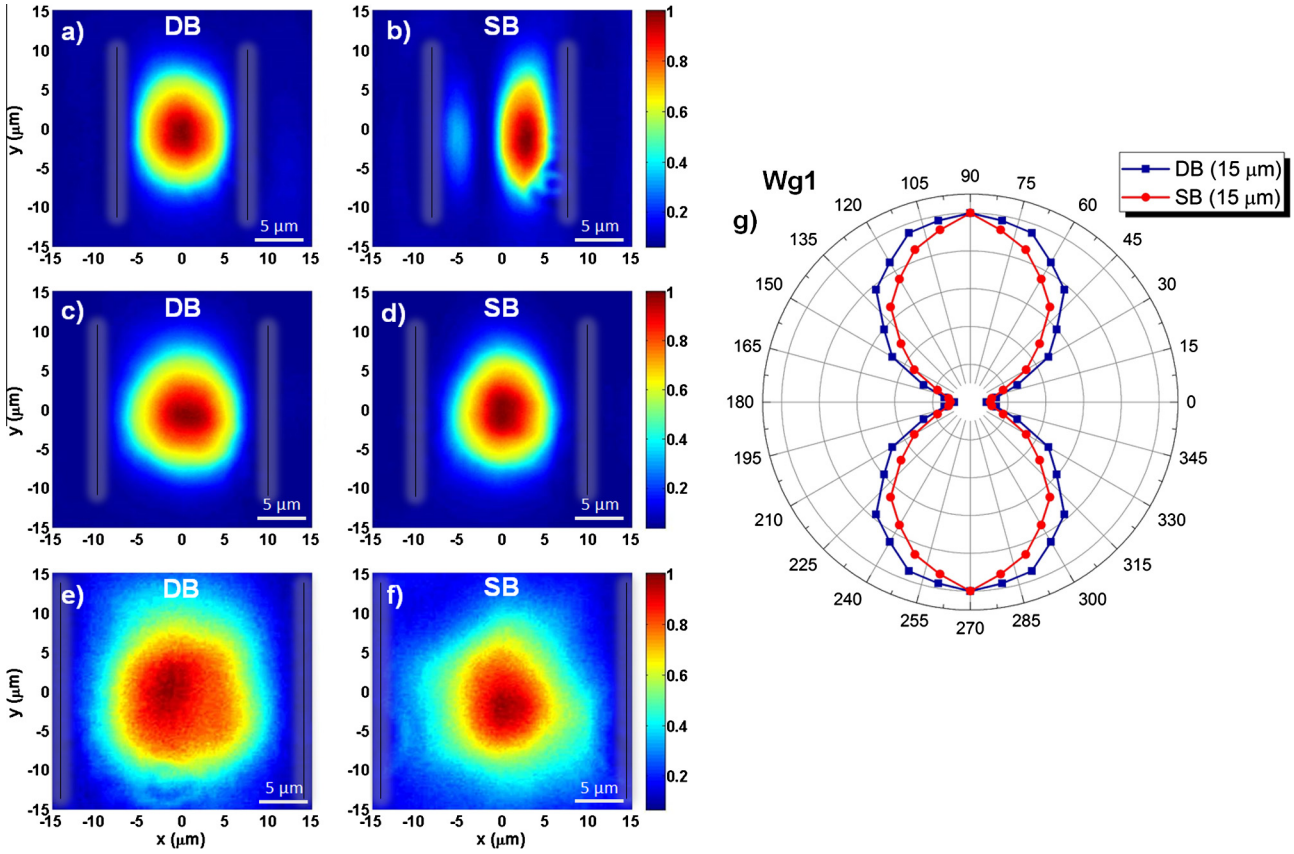

Fig. 2. (a–f) Modal profiles of the waveguides at 633 nm and polarization parallel to the damage tracks (approximate positions shown by vertical lines). (a and b) WG1 (15 μm track separation, 0.44 μJ pulse energy and 25 μm/s scanning velocity) for DB and SB fabrication, (c and d) WG2 (20 μm track separation and same irradiation conditions), and (e and f) WG3 (30 μm track separation, 0.90 μJ pulse energy and 100 μm/s scanning velocity). (g) Polarization dependence of the transmitted power (normalized) for WG1 (0° corresponds to polarization perpendicular to damage tracks).

index contrast (Δn) between the damage lines (refractive index decrease) and the waveguide core (refractive index increase induced by the stress field) was estimated by measuring the numerical aperture of the guided mode in the far-field. Then, assuming in a rough estimation a step-index profile, the refractive index contrast was calculated using the equation [22]

$$\Delta n \approx \frac{\sin^2 \theta_m}{2n}, \quad (1)$$

where θ_m is the maximum incident angle at which the transmitted power occurs without any change, while n, in a first approximation, is the refractive index of the bulk material.

2.3. Micro-luminescence measurements

Micro-luminescence imaging of the stress-induced waveguides were obtained in a home-made confocal fluorescence microscope. A single-mode fiber coupled laser diode (808 nm) was used as an excitation source. It was focused into the sample by using a single microscope objective with a numerical aperture of 0.85, leading to an excitation laser spot radius of 0.5 μm approximately. 808 nm radiation excites Nd^{3+} ions from their ground state ($^4I_{9/2}$) up to their $^4F_{5/2}$ excited state from which non radiative de-excitations down to the $^4F_{3/2}$ metastable state take place. The subsequent $^4F_{3/2} \rightarrow {}^4I_{9/2}$ emission is collected by the same microscope objective and, after passing through different spectral and spatial filters is spectrally analyzed by a high-resolution spectrometer. In this work we focused our attention to the spatial variation of the intensity, spectral position and bandwidth of the narrow emission lines centered at around 940 nm as they have been demonstrated in the past to be excellent indicators of the local damage, stress and disorder in the Nd:YAG network, respectively [10]. For the acquisition of fluorescence and structural images of the waveguides, the Nd:YAG sample was scanned in three dimensions by placing it on an XYZ piezo-stage while keeping the 808 nm excitation spot fixed. The spatial variation of peak intensity, position and width (used for damage, stress and disorder imaging) were obtained by using the LabSpec software. Graphical representation of data was performed by using the WSxM software [23].

3. Results and discussion

Firstly, the modal profiles of the fabricated waveguides were analyzed. Guidance was observed for the three track separations but the fabrication parameters (pulse energy/scanning velocity) that minimized the measured losses were different (see Fig. 2): 0.44 μJ/25 μm/s for 15 μm (WG1) and 20 μm (WG2) track separation, and 0.90 μJ/100 μm/s for 30 μm track (WG3) separation. As it can be seen in the figure, the modal profiles for DB waveguides were highly symmetrical and single mode in all the cases. However, SB waveguides show more irregular profiles, effect that is particularly noticeable for small track separations for which asymmetric multimode profiles are obtained.

Concerning the propagation losses, in all the measurements DB waveguides showed superior performance with a loss reduction between 5% and 30% with respect to SB waveguides. In particular, propagation loss as low as ~0.2 dB/cm was measured for the DB-WG2 and ~0.3 dB/cm for SB-WG2. This value obtained for DB

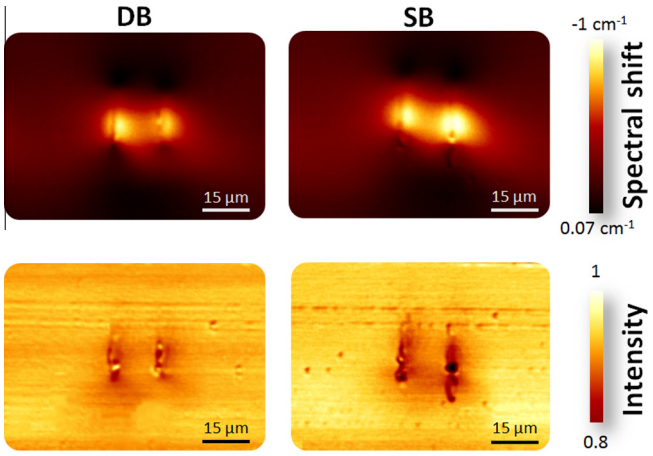

Fig. 3. Micro-luminescence maps of WG1 obtained by DB (left) and SB (right) inscription. Top panels show the spatial variation of the stress-induced spectral shift of Nd:YAG emission lines. These maps clearly reveal a larger symmetry of the stress-field pattern in the case of DB inscription. Bottom panels represent the spatial distribution of the Nd:YAG luminescence intensity that is related to the spatial variation of laser-induced damage in the Nd:YAG crystal lattice.

waveguides improves previously reported values for Nd:YAG stress-induced waveguides [12]. However, the refractive index contrast estimated from Eq. (1) was larger for the SB waveguide $\sim 8 \cdot 10^{-4}$ (DB waveguide $\sim 4 \cdot 10^{-4}$). This behavior is surprising, as one would expect a larger refractive index contrast induced in the material when two mechanical waves (compressive) were produced simultaneously from both damage tracks to the center of the waveguide. Nevertheless this effect could be tentatively explained taking into account that the refractive index change here estimated should be considered as an average value in the whole waveguide. In the case of SB irradiation, the second damage track is produced on a pre-modified volume of the YAG network so a larger modification (refractive index change) would be expected, this leading to a larger "overall" refractive index change.

The effect of the incident laser polarization on the supported waveguide modes was also investigated. In all the cases, the guidance is better for polarization parallel to the damage tracks and poor for the perpendicular one, although a slightly more isotropic behavior is found for DB waveguides (see as example Fig. 2g).

To gain insight in the mechanisms underlying the different behaviors observed, luminescence maps were taken for the different waveguides. In Fig. 3 we show the peak position (Top panel) and intensity (Bottom panel) maps corresponding to WG1 (15 μm track separation). As explained in detail in previous references (see [10]) these maps can be unequivocally correlated to the spatial distribution of residual stress and damage, respectively. Independently on the inscription method, the double filament structures are characterized by a localized damage at the filaments that is accompanied by a compressive stress at filaments and in their surroundings (such compressive stress is denoted by a red-shift in the emission lines). This fact indicates that in both inscription procedures the mechanism leading to waveguide formation is the same: the refractive index increment created at filaments and between them due to compressive stress.

However, clear differences can be appreciated: as it is expected, the simultaneous irradiation (DB) to produce both damage tracks leads to a more symmetrical stress field and, also, to a more similar damage distribution in both tracks of the waveguide. Such creation of highly symmetrical stress patterns leads, consequently, to a more symmetrical refractive index increase distribution in all the studied cases. In the standard double-scan approach (SB) the stress field is asymmetric due to the presence of the so-called "incubation" effect: the inscription of the first damage track leads to the appearance of a modified volume in the Nd:YAG that is not only restricted to the laser focal volume but that, indeed, extends several microns from it. Then, the inscription of the second damage filament is not performed on an "unperturbed" Nd:YAG volume (as it was in the case of the first filament) but, on the contrary, it is performed on a "pre-modified" Nd:YAG lattice so that the resulting structural effects (stress, damage and disorder) are completely different [9]. This effect is particularly relevant for small track separations. This makes both inscription methods non-equivalent leading to the appearance of asymmetrical structural maps and, hence, to asymmetrical refractive index patterns. Thus, in such case, only certain irradiation conditions lead to symmetrical modal profiles (see Fig. 2d). The effect of the SB fabrication in two subsequent sample scans affects even to the different aspect ratio and vertical positions of the damage tracks, as it can be seen in the microscope images shown in a number of papers (see for instance [9–14]). On the other hand, a more homogeneous stress distribution in the volume between the damage tracks is produced with DB irradiation, what means a more uniform refractive index increase in the waveguide region. This behavior could explain the greater extension observed in the modal profiles of DB waveguides. In such case, the reported estimations of the refractive index contrast for both DB and SB waveguides (based on Eq. (1)) would not lead to comparable values as they correspond to very different index profiles.

4. Conclusions

In conclusion, we have presented an study of stress-induced waveguides fabricated in Nd:YAG by simultaneous double beam irradiation with femtosecond pulses. The setup is based on an interferometer that allows the perfect equalization of the energy of the two beams, the adjustment of delay 0 between them, and the fine control of the separation between focal spots. The waveguides fabricated in this approach are compared to those fabricated with the "traditional" double scan technique (SB), and the modal profiles and optical performances are different in both cases. The stress field (derived from micro-luminescence maps) induced with simultaneous (DB) irradiation is symmetrical, leading to symmetrical, monomode and larger modal profiles in all the studied irradiation conditions. Moreover, with DB irradiation a significant reduction of propagation losses was achieved. Measurements performed on the numerical aperture of the waveguides report that SB technique produces a larger refractive index contrast in comparison to the DB. However, the different refractive-index profiles that are expected in both waveguide approaches make these estimations difficult to compare.

Acknowledgements

This work was supported by the Ministerio de Economía y Competitividad under Projects FIS2013-44174-P and MAT2013-47395-C4-1-R. The femtosecond laser inscription was carried out in the Spanish Pulsed Laser Center (CLPU) with their Laser Service (High-Repetition-Rate laser system) and their technical assistance, in the framework of the access agreement concerning USAL staff.

References

[1] G. Lifante, Integr. Photon. (2003), http://dx.doi.org/10.1002/0470861401.
[2] R.R. Gattass, E. Mazur, Femtosecond laser micromachining in transparent materials, Nat. Photon. 2 (2008) 219–225, http://dx.doi.org/10.1038/nphoton.2008.47.
[3] L. Cerami, E. Mazur, S. Nolte, C.B. Schaffer, Femtosecond. Laser Micromach. (2013), http://dx.doi.org/10.1007/978-3-642-23366-1.
[4] F. Chen, J.R. Vázquez de Aldana, Optical waveguides in crystalline dielectric materials produced by femtosecond-laser micromachining, Laser Photon. Rev. 8 (2014) 251–275, http://dx.doi.org/10.1002/lpor.201300025.

[5] D. Choudhury, J.R. Macdonald, A.K. Kar, Ultrafast laser inscription: perspectives on future integrated applications, Laser Photon. Rev. 8 (2014) 827–846, http://dx.doi.org/10.1002/lpor.201300195.
[6] K. Sugioka, Y. Cheng, Ultrafast lasers—reliable tools for advanced materials processing, Light Sci. Appl. 3 (2014) e149, http://dx.doi.org/10.1038/lsa.2014.30.
[7] C.B. Schaffer, A. Brodeur, E. Mazur, Laser-induced breakdown and damage in bulk transparent materials induced by tightly focused femtosecond laser pulses, Meas. Sci. Technol. 12 (2001) 1784–1794, http://dx.doi.org/10.1088/0957-0233/12/11/305.
[8] S. Gross, M. Dubov, M.J. Withford, On the use of the Type I and II scheme for classifying ultrafast laser direct-write photonics, Opt. Expr. 23 (2015) 7767, http://dx.doi.org/10.1364/OE.23.007767.
[9] J. Burghoff, H. Hartung, S. Nolte, A. Tünnermann, Structural properties of femtosecond laser-induced modifications in $LiNbO_3$, Appl. Phys. A 86 (2006) 165–170, http://dx.doi.org/10.1007/s00339-006-3750-6.
[10] A. Ródenas, G.A. Torchia, G. Lifante, E. Cantelar, J. Lamela, F. Jaque, et al., Refractive index change mechanisms in femtosecond laser written ceramic Nd:YAG waveguides: micro-spectroscopy experiments and beam propagation calculations, Appl. Phys. B 95 (2009) 85–96, http://dx.doi.org/10.1007/s00340-008-3353-3.
[11] G.A. Torchia, A. Rodenas, A. Benayas, E. Cantelar, L. Roso, D. Jaque, Highly efficient laser action in femtosecond-written Nd:yttrium aluminum garnet ceramic waveguides, Appl. Phys. Lett. 92 (2008) 111103, http://dx.doi.org/10.1063/1.2890073.
[12] J. Siebenmorgen, K. Petermann, G. Huber, K. Rademaker, S. Nolte, A. Tünnermann, Femtosecond laser written stress-induced Nd:$Y_3Al_5O_{12}$ (Nd:YAG) channel waveguide laser, Appl. Phys. B 97 (2009) 251–255, http://dx.doi.org/10.1007/s00340-009-3697-3.
[13] W.F. Silva, C. Jacinto, A. Benayas, J.R. Vazquez de Aldana, G.A. Torchia, F. Chen, et al., Femtosecond-laser-written, stress-induced Nd:YVO_4 waveguides preserving fluorescence and Raman gain, Opt. Lett. 35 (2010) 916–918, http://dx.doi.org/10.1364/OL.35.000916.
[14] C. Zhang, N. Dong, J. Yang, F. Chen, J.R. Vázquez de Aldana, Q. Lu, Channel waveguide lasers in Nd:GGG crystals fabricated by femtosecond laser inscription, Opt. Expr. 19 (2011) 12503–12508, http://dx.doi.org/10.1364/OE.19.012503.
[15] J. Burghoff, C. Grebing, S. Nolte, A. Tünnermann, Efficient frequency doubling in femtosecond laser-written waveguides in lithium niobate, Appl. Phys. Lett. 89 (2006) 081108, http://dx.doi.org/10.1063/1.2338532.
[16] F. Laurell, T. Calmano, S. Müller, P. Zeil, C. Canalias, G. Huber, Laser-written waveguides in KTP for broadband Type II second harmonic generation, Opt. Expr. 20 (2012) 22308, http://dx.doi.org/10.1364/OE.20.022308.
[17] S.J. Beecher, R.R. Thomson, D.T. Reid, N.D. Psaila, M. Ebrahim-Zadeh, A.K. Kar, Strain field manipulation in ultrafast laser inscribed BiB3O6 optical waveguides for nonlinear applications., Opt. Lett. 36 (2011) 4548–4550. <http://www.ncbi.nlm.nih.gov/pubmed/22139238>.
[18] S. Müller, T. Calmano, P. Metz, N.-O. Hansen, C. Kränkel, G. Huber, Femtosecond-laser-written diode-pumped Pr:LiYF4 waveguide laser, Opt. Lett. 37 (2012) 5223–5225, http://dx.doi.org/10.1364/OL.37.005223.
[19] H. Liu, J.R. Vázquez de Aldana, B. del Rosal Rabes, F. Chen, Waveguiding microstructures in Nd:YAG with cladding and inner dual-line configuration produced by femtosecond laser inscription, Opt. Mater. (Amst). 39 (2015) 125–129, http://dx.doi.org/10.1016/j.optmat.2014.11.010.
[20] S. Nolte, J. Burghoff, M. Will, A. Tuennermann, Femtosecond writing of high-quality waveguides inside phosphate glasses and crystalline media using a bifocal approach, Commer. Biomed. Appl. Ultrafast Lasers IV. 5340 (2004) 164–171, http://dx.doi.org/10.1117/12.537365.
[21] J.F. Bourhis, Fibre to waveguide connection, in: S.I. Najafi (Ed.), Glass Integrated Optics and Optical Fiber Devices of the Critical Reviews of Optical Science and Technology, SPIE, 1994.
[22] J. Siebenmorgen, T. Calmano, K. Petermann, G. Huber, Highly efficient Yb:YAG channel waveguide laser written with a femtosecond-laser, Opt. Expr. 18 (2010) 16035–16041, http://dx.doi.org/10.1364/OE.18.016035.
[23] I. Horcas, R. Fernández, J.M. Gómez-Rodríguez, J. Colchero, J. Gómez-Herrero, a. M. Baro, WSXM: a software for scanning probe microscopy and a tool for nanotechnology, Rev. Sci. Instrum. 78 (2007) 013705, http://dx.doi.org/10.1063/1.2432410.